

## Percolation in one of $q$ colors near criticality

Xiaofeng Qian,<sup>1</sup> Youjin Deng,<sup>2,\*</sup> and Henk W. J. Blöte<sup>1,2</sup>

<sup>1</sup>*Lorentz Institute, Leiden University, P.O. Box 9506, 2300 RA Leiden, The Netherlands*

<sup>2</sup>*Faculty of Applied Sciences, Delft University of Technology, P.O. Box 5046, 2600 GA Delft, The Netherlands*

(Received 1 March 2005; published 29 April 2005)

We study bond percolation in two dimensions between random site variables having one out of  $q$  colors, using transfer-matrix and Monte Carlo techniques. We determine the percolation threshold as a function of the Potts temperature  $T$  in the disordered Potts range  $T_c \leq T < \infty$  for several  $q$ -state Potts Hamiltonians. For high  $T$ , these transitions fit, irrespective of  $q$ , in the universality class of the ordinary percolation transitions. However, for  $T \downarrow T_c$ ,  $q$ -dependent crossover phenomena appear. The topology of the phase diagram changes in a qualitative sense at  $q=2$ . For  $q < 2$  the Potts critical state appears to enhance percolation, for  $q > 2$  it appears to suppress it. Remarkably, for  $q=2$  the percolation line coincides with the *only* flow line extending to  $T > T_c$  from the critical fixed point associated with Potts clusters.

DOI: 10.1103/PhysRevB.71.144303

PACS number(s): 05.50.+q, 64.60.Cn, 64.60.Fr, 75.10.Hk

### I. INTRODUCTION

The universal properties of the pure percolation problem in two dimensions are well understood. While short-range correlations in the substrate do not influence the universality class of the percolation transition, percolation phenomena on critical substrates display new universal behavior. Such correlated percolation models have already been the subject of various investigations. For instance, motivated by the prospect to find new types of critical behavior, the study of percolation phenomena in  $q$ -state Potts configurations has received considerable attention;<sup>1–6</sup> see also references therein. The correlated percolation problem, while interesting in its own right, is also relevant for a several other fields of research, see for instance Refs. 7–9, and references therein. These fields include colossal magnetoresistance, correlated resistor networks and the quantum-Hall transition.

The reduced Hamiltonian of the  $q$ -state Potts model is

$$\mathcal{H}/k_B T = -K \sum_{\langle ij \rangle} \delta_{\sigma_i, \sigma_j}, \quad (1)$$

with Potts variables  $\sigma_i (= 1, 2, \dots, q)$ , and  $\langle ij \rangle$  runs over all interacting pairs of such variables. The Kasteleyn-Fortuin mapping<sup>10</sup> of Eq. (1) on the random-cluster model generalizes it to continuous  $q$ . This mapping involves the formation of percolation clusters: each pair  $(ij)$  with  $\sigma_i = \sigma_j$  is connected by a bond  $b_{ij} = 1$  with probability  $p = 1 - e^{-K}$ . After summing out the Potts variables, only bond variables remain in the partition sum

$$Z(q; K) = \sum_{\{b\}} u^{n_b} q^{n_c}, \quad (2)$$

where the sum is on all  $b_{ij} = 0, 1$ ;  $u \equiv e^K - 1$ ,  $n_b$  is the number of bonds, and  $n_c$  the number of clusters. The percolation threshold of the random-cluster model appears to coincide with the Potts critical point, and the critical exponents describing its percolation and thermodynamic properties appear to depend continuously on  $q$ .

While the bond percolation probability  $p$  in the random-cluster model is determined by the Potts coupling  $K$ , here we consider the more general case that  $p$  is independent of  $K$ . Since all Potts colors are equivalent, it is sufficient to form clusters of one color, say  $\sigma_i = 1$ . These sites are considered “occupied” and percolation bonds are added between occupied sites with probability  $p$ . The resulting partition sum

$$Z = \left[ \prod_k \sum_{\sigma_k=1}^q \right] \left[ \prod_{\langle ij \rangle} \exp(K \delta_{\sigma_i, \sigma_j}) \sum_{b_{ij}=0}^1 \{1 - b_{ij} + p(2b_{ij} - 1) \times \delta_{\sigma_i, 1} \delta_{\sigma_j, 1}\} \right] \quad (3)$$

is equal to the Potts partition sum, but its terms include percolation degrees of freedom. Two special cases are (1)  $p=1$ , leading to so-called Potts clusters, and (2)  $p=1 - e^{-K}$  reproducing random clusters.<sup>10</sup> Most work has thus far focused on these two cases at the Potts critical point  $K=K_c$ .<sup>1–6</sup> The results for the Ising case  $q=2$  in terms of the phase diagram and the renormalization flow are summarized in Fig. 1. The qualitative characteristics are, however, believed to apply more generally than just for  $q=2$ . Along the critical line  $K=K_c$  the bond probability is relevant at the random-cluster fixed point. The flow in the  $p$ -direction is governed by the so-called red-bond exponent.<sup>2</sup> Thus we expect stable fixed points on either side. A trivial fixed point naturally occurs at  $p=0$ , but the location of the stable fixed point at  $p_s > 1 - e^{-K}$  is not well known. Furthermore, there are fixed points at infinite Potts temperature  $K=0$ , of which we mention the fully stable trivial one at  $p=0$ , and the one at the percolation threshold  $p_c$ . The latter fixed point is thus unstable in the  $p$ -direction. It describes a mixed site-bond percolation problem where sites are occupied with probability  $1/q$ .

In particular the percolation phenomena at and near Potts criticality remain largely unexplored. It is therefore the subject of this paper to determine how the  $K=0$  percolation transition continues for  $K > 0$ , how it connects to the critical line  $K=K_c$ , and how the resulting phase diagram and its un-

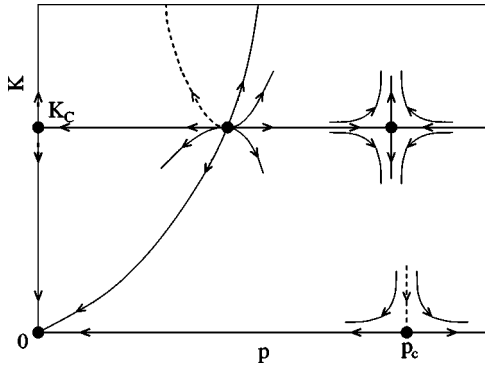


FIG. 1. The  $(p, K)$  diagram. The curve connecting to  $K=p=0$  represents the random-cluster model. Arrows indicate the renormalization flow. Dashed lines show the percolation threshold in the ordered phase ( $K > K_c$ ) and for small  $K$ .

derlying flow-line structure depend on the number of Potts states  $q$ . The outline of this paper is as follows. In Sec. II we summarize the numerical techniques and describe the determination of the critical points needed in the following calculations. Sections III and IV present our results for the Ising case  $q=2$ , and for  $q \neq 2$  respectively. Section V concludes this paper with a brief discussion and an investigation of some remaining questions.

## II. ALGORITHMS AND CRITICAL POINTS

### A. Critical points

The critical couplings  $K_c$  of the models that are investigated in the following sections, are available from various sources including exact analysis, duality transformations, transfer-matrix calculations and Monte Carlo simulations. First, the critical point of the nearest-neighbor Potts model on the square lattice is known from duality<sup>11</sup> as  $K_c = \ln(1 + \sqrt{q})$ . The transformation<sup>10</sup> of the Potts partition sum into a Whitney polynomial, which is self-dual,<sup>12</sup> enables the generalization of this result to noninteger  $q$ . The critical point of the exactly solved<sup>13</sup> triangular  $q=2$  model is  $K_c = \ln(3)/2$ .

The determination of the critical points of the other systems investigated requires the use of numerical means. The square-lattice Ising model with eight equivalent neighbors has been analyzed by means of a transfer-matrix method.<sup>14</sup> In terms of the Potts coupling (which is twice the coupling in the equivalent Ising Hamiltonian) the critical point is thus known as  $K=0.3803853614(4)$ .

The models with many more interacting neighbors are less easy to investigate by transfer-matrix methods, and Monte Carlo methods were used instead. There exists an efficient cluster algorithm<sup>15</sup> for such models: critical slowing down is strongly reduced, and the time per spin flip is almost independent of the number of interacting neighbors. The determination of the critical point is based on the Monte Carlo sampling of the moments of the magnetization  $m$  and the determination of their dimensionless ratio  $Q \equiv \langle m^2 \rangle^2 / \langle m^4 \rangle$ , which is related to the Binder cumulant<sup>16</sup> and converges to a universal constant at the critical point in the limit of large

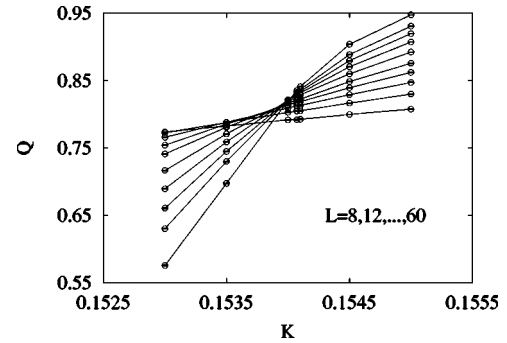


FIG. 2. Dimensionless ratio  $Q$  of the 20-neighbor 3-state Potts model versus coupling  $K$ , for several system sizes. Data points (circles) for the same system size are connected by lines. Larger system sizes correspond to larger slopes.

system size  $L$ . Multivariate least-squares analysis of Monte Carlo results for  $Q$ , obtained in a narrow interval around the critical point for a sequence of different sizes  $L$ , then yields the critical point. This procedure was described in Ref. 17 and applied there to several equivalent-neighbor Ising models on the square lattice. We quote its result for the 20-neighbor Ising model, in terms of the Potts coupling, as  $K_c = 0.1263852(8)$ .

For the three-state Potts model on the square lattice with 20 equivalent neighbors we performed new simulations to determine the critical point. The density  $n_\sigma$  of Potts variables in state  $\sigma$  ( $=1, 2$ , or  $3$ ) was sampled for 20 system sizes in the range  $8 \leq L \leq 200$ . The quantity  $Q$  is now defined as above but with  $m^2$  replaced by  $[(n_1 - n_2)^2 + (n_2 - n_3)^2 + (n_3 - n_1)^2] / 2$ . The data for system sizes  $L \leq 60$  are shown in Fig. 2. The apparent converge of the intersections hints at a phase transition near  $K=0.154$ . Multivariate least-squares analysis of  $Q$ , along the lines of Ref. 17, but with the Ising correction-to-scaling exponents replaced by the three-state Potts ones, yielded the critical point as  $K_c = 0.154078(1)$ . The fit was able to resolve the temperature exponent  $y_t$  which was found to agree well with the three-state Potts universality class. This result confirms that the transition is continuous. In contrast, a first-order transition is predicted by mean-field theory. The predictions of mean-field theory might be considered relevant because they tend to become more accurate when the range of interactions increases.

### B. Percolation algorithms

The percolation problem defined in Sec. I was studied by means of a transfer-matrix technique whose principle was outlined in Ref. 18, and by means of cluster Monte Carlo algorithms for the Potts model<sup>19,20</sup> and for the noninteger- $q$  random-cluster model.<sup>21,22</sup> The transfer-matrix method uses in fact the random-cluster representation of the  $q=1$  Potts model as outlined in Ref. 23. In particular the “magnetic” connectivities defined there serve to construct a transfer matrix that enables the calculation of “magnetic correlations,” i.e., the probability that two sites belong to the same percolation cluster. The fact that we now construct percolation

clusters only between variables in the same state makes it necessary to construct a more complicated algorithm than that used in Ref. 23. These complications were solved in a rather straightforward but tedious way; we do not go into details here.

In contrast, the Monte Carlo construction of percolation clusters between variables in the same state is rather simple; the algorithm is essentially the same as the Wolff algorithm<sup>20</sup> used to generate the Potts configurations for integer  $q$ , but with a different bond probability.

### III. THE ISING CASE $q=2$

First we search for the stable fixed point of the Ising model ( $q=2$ ) at  $K=K_c$ ,  $p>0$ . Reference 18 suggests that the fixed point lies near  $p=1.1$  for the square lattice, but a sketch in Ref. 3 shows it at  $p<1$ . We used the transfer matrix of Ref. 18 to compute the correlation length  $\xi(p,K,L)$  of the probability that two sites at a distance  $r$  along a cylinder of circumference  $L$  belong to the same cluster. From it we define

$$X_h(p,K,L) \equiv \frac{L}{2\pi\xi(p,K,L)}, \quad (4)$$

where  $X_h(p,K,L) \approx X_h$  in the limit of large  $L$ , with  $X_h$  the magnetic scaling dimension at the fixed point attracting the point  $(p,K)$ . We fix  $K=K_c$  and apply finite-size scaling near a stable fixed point at  $p=p_s$ :

$$X_h(p,K_c,L) = X_h(p_s + (p-p_s)L^{y_r}, K_c, 1) + \dots \quad (5)$$

with a red-bond exponent  $y_r = -5/8$ .<sup>18</sup> In first order, corrections to scaling  $X_h(p,K_c,L) - X_h$  are proportional to the irrelevant field  $p-p_s$  and can thus be used to determine  $p_s$ . Using numerical data for  $X_h(p,K_c,L)$  for sizes up to  $L=11$  at several values of  $p$ , and the exact result  $X_h=5/96$ , and a least-squares fit of an expansion of Eq. (5) in  $p-p_s$ , we obtain  $p_s=1.08(3)$ . This bond probability exceeds 1 and is thus unphysical, but there is no sign of a change of universality.

The same algorithm was used to locate percolation transitions for  $K<K_c$ . Near the  $K=0$  percolation fixed point the data for  $X_h$  were fitted by

$$X_h(p,K,L) = X_h + \sum_k a_k (p-p_c)^k L^{ky_p} + \sum_j b_j L^{jy_i} + \dots, \quad (6)$$

where  $X_h=5/48$  is the magnetic dimension and  $y_p=3/4$  the thermal exponent of the percolation model; the irrelevant Potts exponent is  $y_i=-1$  near  $K=0$ . The resulting percolation line is shown in Fig. 3. It lies wholly in the unphysical region. Reasonably accurate data could be obtained for  $K \leq 0.7$ ; for larger  $K$ , the available range of finite sizes is insufficient because of crossover phenomena due to the proximity of the Ising critical point. The percolation line seems to connect to the *irrelevant* fixed point. This is remarkable, because then the percolation line is, among infinitely many flow lines in the  $(p,K)$  diagram for  $K<K_c$ , the only one extending down from the stable fixed point  $(p_s, K_c)$  and the

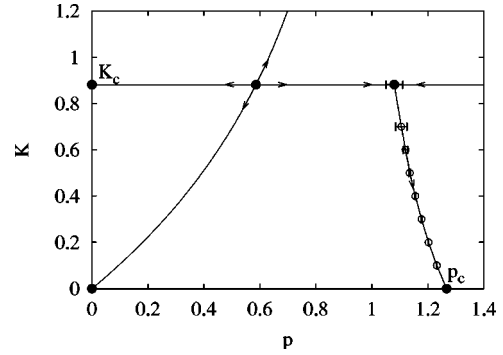


FIG. 3. Percolation diagram of the square-lattice, nearest-neighbor Ising model. The percolation line lies in the unphysical region  $p>1$ . It runs from  $p_c=1.2668(2)$ ,  $K=0$  to the stable fixed point on the critical line  $K=K_c$ .

only flow line coming in to the percolation fixed point  $(p_c, 0)$ . Coincidence of both flow lines (see Fig. 1) hints at a deeper connection involving these two seemingly independent fixed points.

In view of the unexpectedness of this result, we have performed similar analyses of different Ising models. First we studied the  $q=2$  model with eight equivalent neighbors on the square lattice. Its critical point is known as  $K=0.3803853614(4)$ .<sup>14</sup> Because of the increased number of neighbors, the percolation line for  $K<K_c$  shifts into the physical range  $p \leq 1$  where Monte Carlo methods can be applied. For several periodic lattices up to size  $L=360$ , up to  $10^7$  spin configurations were generated by Metropolis or Wolff<sup>20</sup> methods, and percolation clusters were formed. For a range of values of  $p$  and  $K$ , we then sampled the dimensionless ratio

$$Q = \frac{\langle \sum_i c_i^2 \rangle^2}{\langle 3(\sum_i c_i^2)^2 - 2\sum_i c_i^4 \rangle}, \quad (7)$$

where  $c_i$  is the size of the  $i$ th cluster. In the Ising case  $q=2$ , the sum over *all* random clusters (i.e.,  $p=1-e^{-K}$ ) yields a result that is equal to the above-mentioned ratio of magnetization moments  $Q = \langle m^2 \rangle^2 / \langle m^4 \rangle$ . However, here the sum includes clusters of *only one* Potts color, to ensure that  $Q$  satisfies universality independent of  $q$ . Near the percolation threshold it scales as

$$Q = Q_0 + \sum_k a_k (p-p_c)^k L^{ky_p} + \sum_{j=1,2,\dots} b_j L^{jy_i} + c(p-p_c)L^{y_p+y_i} + d(p-p_c)^2 L^{y_p} + eL^{y_p-2y_h} + fL^{d-2y_h} + \dots \quad (8)$$

with  $y_p=3/4$ ,  $y_h=91/48$ ,  $y_i=-1$ , and  $Q_0=0.87048(5)$ . We determined this value of  $Q_0$  numerically for the square-lattice bond-percolation model, prior to the present analysis. Meanwhile an independent determination of  $Q_0$  has appeared in Ref. 24. Corrections to the leading scaling behavior are due to the analytic background, nonlinearity of the relevant scaling field in  $p$ , and mixed contributions of other scaling fields to the temperaturelike variable. For  $K \neq 0$ , new corrections may appear due to the correlation between the spin variables.

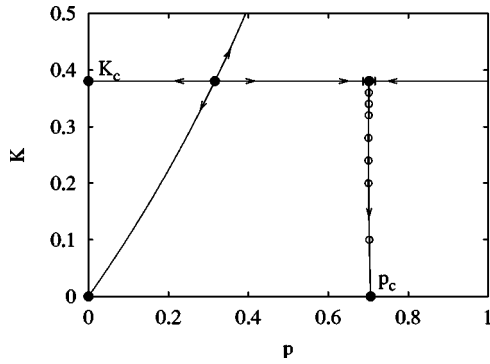


FIG. 4. Percolation diagram of the Ising model on the square lattice with nearest- and next-nearest-neighbor interactions. The percolation line lies in the physical region  $p < 1$ . It runs from  $p_c = 0.70622(6)$  at  $K = 0$  to the stable fixed point at  $p_s = 0.702(15)$  on the critical line  $K = K_c$ .

These are governed by the irrelevant exponent  $y_i = -1$  governing the flow to the infinite-temperature fixed point ( $p = p_c, K = 0$ ).

In order to locate the percolation line, we have fitted the free parameters in formula (8) to our simulation data for  $Q$  at couplings  $K < K_c$ . This procedure was also applied to locate the stable fixed point at  $K = K_c$ , with a different universal value of  $Q_0$ , and with  $y_p$  replaced by the irrelevant exponent  $y_r = -5/8$ . We used the geometric cluster algorithm<sup>25</sup> at zero magnetization, to suppress corrections that obstruct the determination of the fixed point and the error estimation. We verified our results with consistency checks using other definitions of  $Q$ , excluding the largest or second largest cluster, using only the largest cluster, or using two colors instead of one. As shown in Fig. 4, again the percolation line approaches the stable fixed point.

We have similarly analyzed the triangular Ising model. As shown in Fig. 5, we find a percolation line at  $p = 1$ . This is explained by an exact argument. The site percolation threshold is  $p_s = 1/2$  (Ref. 26) for the triangular lattice. Thus the present bond percolation model is critical at  $K = 0, p = 1$ . However, the “matching lattice” argument<sup>26</sup> behind this result requires only that the site probability distribution is symmetric under the interchange of occupied and empty sites. Thus, the present triangular percolation model is still critical

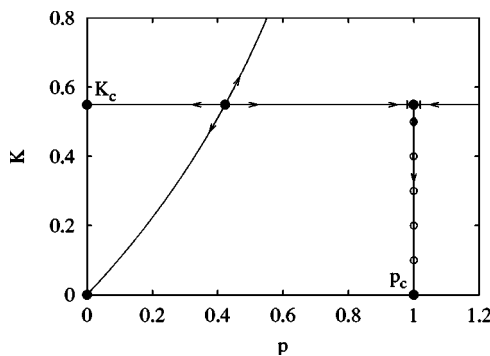


FIG. 5. Percolation diagram of the triangular Ising model with nearest-neighbor interactions. The percolation line lies exactly at  $p = 1$ .

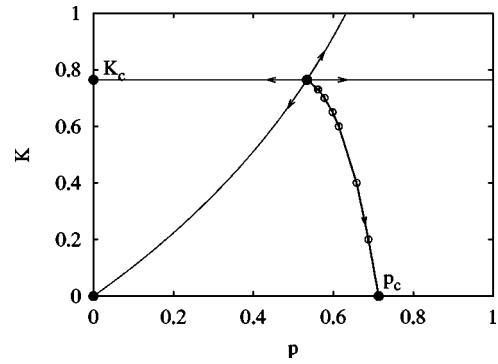


FIG. 6. Percolation diagram of the  $q = 2 - 2 \cos(7\pi/18)$  Potts model on the square lattice with nearest-neighbor interaction. The percolation line runs from  $p_c = 0.71362(2)$ ,  $K = 0$  to the random-cluster fixed point. We did not locate the stable fixed point  $p_s$  on the critical line; interpolation between  $q = 1$  ( $p_s = 1$ ) and  $q = 2$  (see Fig. 3) suggests that it lies in the unphysical range  $p > 1$ .

at  $p = 1$  for  $0 < K \leq K_c$ . For  $K > K_c$  the symmetry is broken and the model is no longer critical.

#### IV. POTTS MODELS WITH $q \neq 2$

This section addresses the question how the phase diagram depends on  $q$ . For  $q = 1$ ,  $K$  is redundant, and the percolation line lies at constant  $p$  and connects to the random-cluster point, i.e., the *unstable* fixed point at  $K = K_c$ . We also studied the square-lattice model at an intermediate value  $q = 2 - 2 \cos(7\pi/18) = 1.31596 \dots$  with a cluster Monte Carlo algorithm<sup>21,22</sup> for the random-cluster model. The cluster decomposition and the analysis are the same as above. The results in Fig. 6 show that, just as for  $q = 1$ , the percolation line connects to the random-cluster point.

Next, we focus on the three-state Potts model. Because of the lower density of sites of one color in the disordered Potts phase, the percolation line of the nearest-neighbor model moves even farther into the unphysical region than in the case of the Ising model. However, the stable fixed point on the critical line  $K = K_c = \ln(1 + \sqrt{3})$  still lies in the physical range at  $p_s = 0.83(2)$ , as determined by the transfer-matrix technique. In order to bring the percolation line into the physical range, we included couplings with a substantial number of neighbors; we adopted the square lattice model with 20 equivalent neighbors, which has its critical point at  $K_c = 0.154078(1)$  as mentioned in Sec. II. We determined the location of the percolation transition line for  $K < K_c$ , and the location of the stable fixed point by an analysis as described above. The results, shown in Fig. 7, indicate that the percolation line does not connect to the stable fixed point located at  $p_s = 0.25(2)$ , but moves to larger  $p$  when  $K \uparrow K_c$ . It seems plausible that the percolation line connects to an unstable fixed point at larger  $p$ , but analysis of our numerical results for the ratio  $Q$  in the physical range  $p \leq 1$  did not reveal clear evidence for such a fixed point.

#### V. DISCUSSION AND MISCELLANEOUS RESULTS

The behavior of the percolation line for  $q = 3$  in the preceding section suggests that the percolation line connects

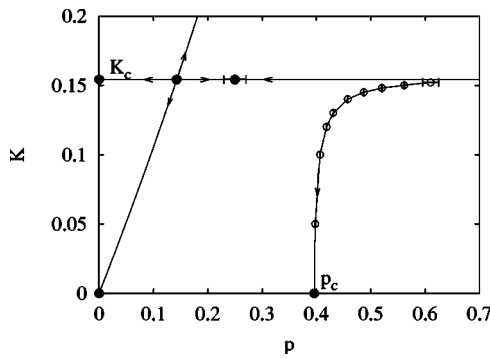


FIG. 7. Percolation diagram of the three-state Potts model on the square lattice with 20 equivalent-neighbors. The percolation threshold lies at  $p_c=0.39591(4)$  for  $K=0$ .

to another unstable fixed point at larger  $p$ . Our data indicate that there is no such fixed point in the physical range  $p \leq 1$ .

In view of the possible existence of such a fixed point for  $q=2$ , we have simulated square-lattice systems with 20 equivalent neighbors up to size  $L=600$  at the critical point (see Sec. II)  $K_c=0.1263852(8)$ . Again the percolation line runs toward the  $K=K_c$  stable fixed point, located at  $p_s \approx 0.210(15)$ . Indeed, from an analysis of the ratio  $Q$  in the interval  $0.8 < p \leq 1$ , using Wolff-type simulations, we found a large- $p$ , unstable fixed point, included in Fig. 8. Quantitative analysis is difficult because of large corrections that suggest the presence of an irrelevant exponent  $y_1 \approx -0.4$ . Thus, our results for this new fixed point have a provisional character. Assuming corrections with exponents that are multiples of  $-0.4$ , we locate the fixed point at  $p_u \approx 0.94(2)$ , and the red-bond exponent as  $y_r=0.54(3)$ , close to the exact value  $13/24$  at the random-cluster point. The fractal dimension  $X_h$  of the clusters was estimated from a finite-size analysis of the largest cluster near  $p=0.94$  as  $X_h=0.035(1)$ .

Our results in the preceding sections indicate that the percolation line connects to the stable fixed point at  $K=K_c$  in the whole two-dimensional Ising universality class. This special topology presumably applies only to  $q=2$ . It does not apply to the cases  $q \neq 2$  that we have investigated. The special situation at  $q=2$  is exposed by defining a second bond

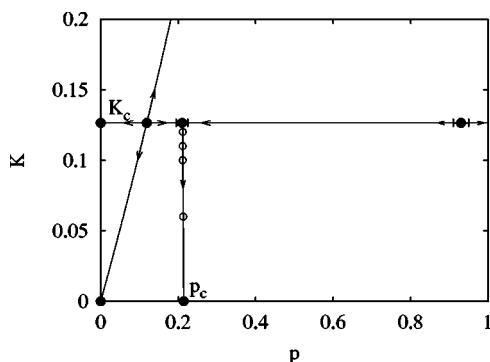


FIG. 8. Percolation diagram of the Ising model on the square lattice with 20 equivalent neighbors. The percolation threshold lies at  $p_c=0.21416(2)$  for infinite temperature  $K=0$ .

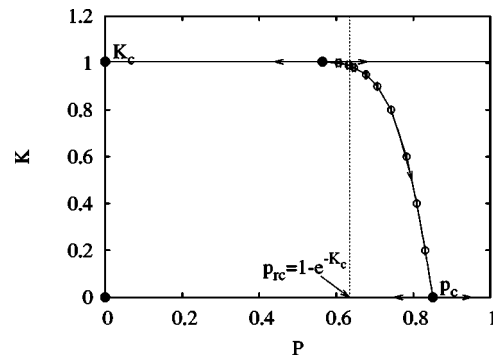


FIG. 9. Percolation diagram of the three-state Potts model on the square lattice, with percolation clusters including variables of two colors. The percolation threshold on the critical line acts as the end point of the percolation line in the disordered phase. It does not coincide with the random-cluster point.

percolation problem between all sites of the  $q-1$  remaining colors. Only for  $q=2$  both problems are equivalent, i.e., there is a symmetry in the model that may force the percolation transitions into a plane parametrized by a zero irrelevant field.

This argument based on symmetry thus predicts that the bond percolation problem involving bonds between sites with *two* out of  $q=3$  colors would lead to a percolation line connecting to the point acting as the percolation threshold on the line  $K=K_c$  (i.e., an unstable fixed point), but which is no longer the random-cluster point. Indeed, our numerical results, for the nearest-neighbor three-state Potts model on the square-lattice, shown in Fig. 9, agree with this prediction. The results yield the percolation threshold at  $K=0$  as  $p_c=0.8509(4)$ : the bond percolation threshold on the square lattice with site probability  $2/3$ . The percolation threshold on the critical line  $K=K_c$  lies at  $p_r=0.5622(2)$ , which is clearly smaller than the random-cluster probability  $p=0.63397 \dots$ .

We conclude this paper by mentioning that the above symmetry argument holds generally for planar lattices only. In three-dimensional systems, percolation between sites with one of  $q$  colors may thus be expected to display different behavior. For instance, for the dilute Ising model at tricriticality, the bond probability  $p$  at the random-cluster fixed point is irrelevant in two dimensions<sup>5</sup> and relevant in three dimensions.<sup>27</sup> Our preliminary simulation results suggest that, in contrast to the two-dimensional case, the one-color-percolation line in the disordered phase of the simple-cubic Ising model connects to the random-cluster fixed point.

ACKNOWLEDGMENTS

We thank J.R. Heringa and H.J.F. Knops for valuable discussions. This research is supported by the Dutch FOM foundation (“Stichting voor Fundamenteel Onderzoek der Materie”) which is financially supported by the NWO (“Nederlandse Organisatie voor Wetenschappelijk Onderzoek”). It was partially done during a visit to the Institute for Mathematical Sciences, National University of Singapore in 2004 which was supported by the Institute.

\*Present address: Laboratory for Materials Science, Delft University of Technology, Rotterdamseweg 137, 2628 AL Delft, The Netherlands.

- <sup>1</sup>M. F. Sykes and D. S. Gaunt, *J. Phys. A* **9**, 2131 (1976).
- <sup>2</sup>A. Coniglio, *Phys. Rev. Lett.* **62**, 3054 (1989).
- <sup>3</sup>C. Vanderzande, *J. Phys. A* **25**, L75 (1992).
- <sup>4</sup>P. J. M. Bastiaansen and H. J. F. Knops, *J. Phys. A* **30**, 1791 (1997).
- <sup>5</sup>Y. Deng, H. W. J. Blöte, and B. Nienhuis, *Phys. Rev. E* **69**, 026114 (2004).
- <sup>6</sup>H.-O. Georgii, O. Häggström, and C. Maes, in *Phase Transitions and Critical Phenomena*, edited by C. Domb and J. L. Lebowitz (Academic, San Diego, 2001), Vol. 18, p. 1.
- <sup>7</sup>P. J. M. Bastiaansen and H. J. F. Knops, *J. Phys. Chem. Solids* **59**, 297 (1998).
- <sup>8</sup>R. A. Römer, "Percolation, Renormalization and the Quantum-Hall Transition," cond-mat/0106004; and in *Computational Statistical Physics From Billiards to Monte-Carlo*, edited by K.-H. Hoffmann and M. Schreiber (Springer, Berlin, 2002).
- <sup>9</sup>J. T. Chalker and P. D. Coddington, *J. Phys. C* **21**, 2665 (1988).
- <sup>10</sup>P. W. Kasteleyn and C. M. Fortuin, *J. Phys. Soc. Jpn.* **46** (Suppl.), 11 (1969); C. M. Fortuin and P. W. Kasteleyn, *Physica* (Amsterdam) **57**, 536 (1972).
- <sup>11</sup>R. B. Potts, *Proc. Cambridge Philos. Soc.* **48**, 106 (1952).
- <sup>12</sup>H. Whitney, *Ann. Math.* **33**, 688 (1932).
- <sup>13</sup>R. M. F. Houtappel, *Physica* (Amsterdam) **16**, 425 (1950).
- <sup>14</sup>M. P. Nightingale and H. W. J. Blöte, *Physica A* **251**, 211 (1998).
- <sup>15</sup>E. Luijten and H. W. J. Blöte, *Int. J. Mod. Phys. C* **6**, 359 (1995).
- <sup>16</sup>K. Binder, *Z. Phys. B: Condens. Matter* **43**, 119 (1981).
- <sup>17</sup>E. Luijten, H. W. J. Blöte, and K. Binder, *Phys. Rev. E* **54**, 4626 (1996).
- <sup>18</sup>H. W. J. Blöte, Y. M. M. Knops, and B. Nienhuis, *Phys. Rev. Lett.* **68**, 3440 (1992).
- <sup>19</sup>R. H. Swendsen and J.-S. Wang, *Phys. Rev. Lett.* **58**, 86 (1987).
- <sup>20</sup>U. Wolff, *Phys. Rev. Lett.* **60**, 1461 (1988).
- <sup>21</sup>L. Chayes and J. Machta, *Physica A* **254**, 477 (1998).
- <sup>22</sup>X. Qian, Y. Deng, and H. W. J. Blöte, *Phys. Rev. E* **71**, 016709 (2005).
- <sup>23</sup>H. W. J. Blöte and M. P. Nightingale, *Physica A* **112**, 405 (1982).
- <sup>24</sup>Y. Deng and H. W. J. Blöte, *Phys. Rev. E* **71**, 016117 (2005).
- <sup>25</sup>J. R. Heringa and H. W. J. Blöte, *Phys. Rev. E* **57**, 4976 (1998).
- <sup>26</sup>J. W. Essam, in *Phase Transitions and Critical Phenomena*, edited by C. Domb and M. S. Green (Academic, London, 1987), Vol. 2, p. 197.
- <sup>27</sup>Y. Deng and H. W. J. Blöte, *Phys. Rev. E* **70**, 056132 (2004).